The mammalian oxysterol-binding protein-related proteins (ORPs) bind 25-hydroxycholesterol in an evolutionarily conserved pocket

Monika SUCHANEK*, Riikka HYNYNEN†, Gerd WOHLFAHRT‡, Markku LEHTO†, Marie JOHANSSON†, Hannu SAARINEN†, Anna RADZIKOWSKA*, Christoph THIELE*[1] and Vesa M. OLKKONEN†[1]

*Max-Planck-Institute of Molecular Cell Biology and Genetics, Pfotenhauerstrasse 108, D-01307 Dresden, Germany, †Department of Molecular Medicine, National Public Health Institute, Biomedicum, P.O. Box 104, FIN-00251 Helsinki, Finland, and ‡Orion Pharma, Computer-Aided Drug Design, P.O. Box 65, FIN-02101 Espoo, Finland

OSBP (oxysterol-binding protein) homologues, ORPs (OSBP-related proteins), constitute a 12-member family in mammals. We employed an *in vitro* [^{3}H]25OH (25-hydroxycholesterol)-binding assay with purified recombinant proteins as well as live cell photo-cross-linking with [^{3}H]photo-25OH and [^{3}H]photoCH (photo-cholesterol), to investigate sterol binding by the mammalian ORPs. ORP1 and ORP2 [a short ORP consisting of an ORD (OSBP-related ligand-binding domain) only] were *in vitro* shown to bind 25OH. GST (glutathione S-transferase) fusions of the ORP1L [long variant with an N-terminal extension that carries ankyrin repeats and a PH domain (pleckstrin homology domain)] and ORP1S (short variant consisting of an ORD only) variants bound 25OH with similar affinity (ORP1L, $K_d = 9.7 \times 10^{-8}$ M; ORP1S, $K_d = 8.4 \times 10^{-8}$ M), while the affinity of GST–ORP2 for 25OH was lower ($K_d = 3.9 \times 10^{-6}$ M). Molecular modelling suggested that ORP2 has a sterol-binding pocket similar to that of *Saccharomyces cerevisiae* Osh4p. This was confirmed by site-directed mutagenesis of residues in proximity of the bound sterol in the structural model. Substitution of Ile^{249} by tryptophan or Lys^{150} by alanine markedly inhibited 25OH binding by ORP2. In agreement with the *in vitro* data, ORP1L, ORP1S, and ORP2 were cross-linked with photo-25OH in live COS7 cells. Furthermore, in experiments with either truncated cDNAs encoding the OSBP-related ligand-binding domains of the ORPs or the full-length proteins, photo-25OH was bound to OSBP, ORP3, ORP4, ORP5, ORP6, ORP7, ORP8, ORP10 and ORP11. In addition, the ORP1L variant and ORP3, ORP5, and ORP8 were cross-linked with photoCH. The present study identifies ORP1 and ORP2 as OSBPs and suggests that most of the mammalian ORPs are able to bind sterols.

Key words: cholesterol, 25-hydroxycholesterol, molecular homology modelling, OSBP-related protein (ORP), oxysterol-binding protein (OSBP), photo-cross-linking.

INTRODUCTION

Families of proteins with homology to the C-terminal ligand-binding domain of OSBP (oxysterol-binding protein) are present in eukaryotic organisms from *Saccharomyces cerevisiae* to human, and have been implicated in various cellular processes such as lipid metabolism, intracellular lipid transport, membrane trafficking and cell signalling [1,2]. In humans, the gene family consists of 12 members, and extensive splice variation increases the number of encoded protein products. The ORPs (OSBP-related proteins) minimally comprise an ORD (OSBP-related ligand-binding domain), but most of them also have an N-terminal portion that typically contains a PH domain (pleckstrin homology domain). The fact that baker's yeast *S. cerevisiae* has seven ORP genes, *OSH1–7* [3], suggests a fundamental role of these genes and their products in the physiology of eukaryotic cells. In accordance with this, each human tissue or cell type expresses a large number of ORPs [4]. Even though most ORP mRNAs are practically ubiquitous, there are marked quantitative tissue- and cell-type-specific differences in their expression [4,5].

OSBP is the most extensively studied member of the ORP protein family. Overexpression of the protein in the presence of its ligand, 25OH (25-hydroxycholesterol) was shown to enhance the synthesis of sphingomyelin [6], but also sterol homoeostasis was affected by excess OSBP [7]. However, a study employing siRNA (small interfering RNA)-mediated knock-down of OSBP expression demonstrated that the protein plays no significant role in maintenance of sterol homoeostasis [8]. The shift of OSBP to a Golgi location upon treatment of cells with 25OH coincides with Golgi translocation and activation of CERT (ceramide transport protein) [9]. The prevailing hypothesis arising from these observations is that OSBP acts as a sterol sensor whose function is to integrate, via regulation of CERT function, the cellular sterol status with sphingomyelin metabolism. Furthermore, OSBP was recently suggested to function as a sterol sensor that controls the dephosphorylation and hence the activity of ERKs (extracellular-signal-regulated kinases) [10]. In addition to OSBP, overexpression of ORP4S or ORP2 (a short ORP consisting of an ORD only) has been reported to impact on cellular sterol, neutral lipid or phospholipid metabolism in cultured cell models [11–13]. In support of ORP function in lipid or sterol metabolism, disruption of the yeast *OSH* genes leads to defects in the intracellular distribution of ergosterol [14], and Osh4p was recently suggested to act as a cytoplasmic sterol carrier [15].

High-resolution structures of Osh4p in complex with five different sterols (cholesterol, ergosterol, 7-hydroxycholesterol, 20-hydroxycholesterol and 25OH) have been solved [16]. The central part of the protein forms a near-complete β-barrel consisting of 19 β-strands in an antiparallel arrangement. A tunnel mainly consisting of hydrophobic residues runs through the barrel forming a sterol-binding pocket. In the presence of bound ligand, the binding pocket is closed by a lid at the N-terminal portion of the protein. Ligand binding stabilizes the closed conformation of the lid, which adopts markedly different conformations

Abbreviations used: DMEM, Dulbecco's modified Eagle's medium; EMEM, Eagle's minimal essential medium; FCS, fetal calf serum; GST, glutathione S-transferase; MBP, maltose-binding protein; 25OH, 25-hydroxycholesterol; OSBP, oxysterol-binding protein; photoCH, photo-cholesterol; ORD, OSBP-related ligand-binding domain; ORP, OSBP-related protein; PH domain, pleckstrin homology domain; PIP, phosphoinositide; wt, wild-type.

[1] Correspondence may be addressed to either of the authors (email thiele@mpi-cbg.de or vesa.olkkonen@ktl.fi).

depending on whether ligand is present or not. In the study by Im et al. [16], a dual function as both sterol transporter and mediator of sterol signals was suggested for Osh4p.

Of the mammalian OSBP/ORP proteins, OSBP and its closest homologue, ORP4, have been shown to bind oxysterols [13,17]. The ligands binding to the ORDs of the remaining family members have so far remained unknown. The ORDs of ORP1, ORP2, ORP9 and ORP10 have been suggested to bind PIPs (phosphoinositides) [11,18–20], but it is unclear whether these interactions involve a pocket such as that found in yeast Osh4p [16]. Identification of ligands for the ORDs of the remaining mammalian ORPs is crucial for elucidation of their functions. Therefore we employed in the present study both an *in vitro* sterol-binding assay and live cell sterol photo-cross-linking to investigate the putative interactions of mammalian ORPs with sterols. Moreover, we carried out molecular modelling and site-directed mutagenesis to study whether the mammalian ORPs have a sterol-binding pocket similar to that of Osh4p.

EXPERIMENTAL

Antibodies and other reagents

Monoclonal antibody against the Xpress epitope was purchased from Invitrogen (Carlsbad, CA, U.S.A.). [^{3}H]PhotoCH (photo-cholesterol) was synthesized as described previously [21]. Photo-25OH; 6-azi-5α-cholestan-3β,25-diol) was synthesized as described by Adams et al. [22]. Oxidation to the 3-oxo-derivative and reduction with [^{3}H]$NaBH_4$ were performed as described by Thiele et al. [21] to obtain [^{3}H]photo-25OH. [^{3}H]25OH was generated by UV irradiation of the photo-25OH, followed by purification of the resulting 25OH by preparative TLC.

Cell culture

COS7 cells were grown in DMEM (Dulbecco's modified Eagle's medium) with 4.5 g/l glucose and sodium pyruvate (DMEM; Sigma–Aldrich, St. Louis, MO, U.S.A.) supplemented with 10 % (v/v) FCS (fetal calf serum), 100 units/ml penicillin and 100 μg/ml streptomycin. HEK-293 cells (human embryonic kidney cells) were grown in EMEM (Eagle's minimal essential medium) with Earle's salts (EMEM; Sigma–Aldrich) supplemented with non-essential amino acids, 10 % FCS and the antibiotics.

cDNA constructs and site-directed mutagenesis

The full-length OSBP/ORP ORFs (open reading frames) used were rabbit OSBP (GenBank® accession no. J05056); human ORP1L (long variant with an N-terminal extension that carries ankyrin repeats and a PH domain) (AF323726), ORP2 (BC000296), ORP3 (NM_015550), ORP6 (AF323728), ORP7 (AF323729), ORP8 (NM_001003712), ORP9 (NM_024586), ORP10 (NM_017784) and ORP11 (NM_022776). Constructs encoding epitope-tagged C-terminal ORDs of OSBP and ORPs 1–11 were created by PCR and encompassed the following amino acid residues of the respective proteins: OSBP, 304–809; ORP1, 514–950; ORP2, 1–480; ORP3, 399–886; ORP4 (NM_030758), 413–916; ORP5 (BC039579), 266–826; ORP6, 426–934; ORP7, 364–842; ORP8, 242–793; ORP9, 268–736; ORP10, 306–764; ORP11, 274–747. For production of fusion proteins in *Escherichia coli*, the rabbit OSBP ORD cDNA was inserted into the BamHI site of pMAL-p2X (New England Biolabs, Ipswich, MA, U.S.A.). Human ORP1L, ORP1S (short variant consisting of an ORD only) (=ORP1 ORD) and ORP2 cDNAs were subcloned into the BamHI site of pGex-1λT (GE Healthcare, Little Chalfont, Bucks., U.K.). Site-directed mutations were introduced in the ORP2 cDNA using the QuikChange® kit (Stratagene, La Jolla, CA, U.S.A.). For live cell photo-cross-linking experiments, all of the cDNAs were subcloned into the pcDNA4HisMaxC expression vector (Invitrogen), which encodes hexahistidine and Xpress™ epitope tags fused at the N-terminus of the insert-encoded proteins. All constructs were verified by sequencing using ABI PRISM BigDye™ Terminator v3.1 Cycle Sequencing kit and ABI3730 DNA analyser (Applied Biosystems, Foster City, CA, U.S.A.).

Homology modelling of human ORP2 structure

The amino acid sequences of all human and mouse ORP proteins as well as those from the yeast *S. cerevisiae* were employed to construct a multiple sequence alignment by using ClustalW (version 1.82) [23]. The structure of yeast Osh4p [16] was used as a template for modelling the ORD of human ORP2. Prime 1.5 (Schrödinger, Portland, OR, U.S.A.) was used to align the ORP2 sequence with Osh4p (PDB code 1zhz) obtained from the RCSB (Research Collaboratory for Structural Bioinformatics at the Department of Chemistry and Chemical Biology and the Center for Molecular Biophysics and Biophysical Chemistry, Rutgers University, Piscataway, NJ, U.S.A.) PDB. Corrections to this alignment were introduced manually, taking the positions of secondary structure elements in the template and the Hidden Markov Model consensus sequence obtained with HMMER/PFAM database (**P**rotein **Fam**ilies Database of Alignments and Hidden Markov Models; http://www.sanger.ac.uk/Software/Pfam/) (integrated into Prime 1.5) into account. The 62 N-terminal residues and the 55-residue insertion, which is remote from the putative sterol-binding site, were omitted from the alignment and the structural model of ORP2. Prime 1.5 was used to build loops for four insertions and two deletion-regions, and after this, new side chains were placed and their conformations optimized. 25OH was taken from the template 1zhz and its position was adjusted in the final minimization of the complete model.

Protein purification from *E. coli*

The MBP (maltose-binding protein)–OSBP ORD and GST (glutathione S-transferase)–ORP1L, ORP1S and ORP2 fusion proteins were produced in *E. coli* BL21(DE3) and purified on Amylose resin (New England Biolabs) or glutathione–Sepharose (GE Healthcare) respectively according to the manufacturers' instructions. Protein concentrations of the specimens were determined by the DC assay (Bio-Rad, Hercules, CA, U.S.A.). Before 25OH binding experiments, the protein preparations were resolved on Laemmli gels, which were stained with Coomassie Blue, scanned and analysed by using the Scion Image software (http://www.scioncorp.com/). According to this, adjustment of the protein amounts added was performed to ensure that the desired concentrations of the full-length fusion proteins were reached.

Charcoal–dextran sterol-binding assay

Binding of [^{3}H]25OH to the purified MBP–OSBP ORD, GST–ORP1L, GST–ORP1S and GST–ORP2 was assayed as described previously [24]. Briefly, the purified proteins (MBP–OSBP ORD at 0.1 μM, the others at 1 μM) were incubated overnight at +4 °C with 5, 10, 20, 40 and 80 nM [^{3}H]sterol in the absence or presence of a 40-fold excess of unlabelled 25OH. The free sterol was thereafter removed with charcoal–dextran, and the protein-bound [^{3}H]sterol remaining in the supernatant was analysed by liquid scintillation counting. K_d values were determined by Scatchard analysis.

Lipid analysis

COS7 cells were grown for 20 h in the presence of 0.2 mCi of [^{3}H]photoCH complexed with β-methylcyclodextrin or for 2 h in the presence of 0.2 mCi of an ethanolic solution of [^{3}H]photo-25OH. The cells were then washed extensively with PBS, UV-irradiated as above, and lipids were extracted with chloroform–methanol according to the Bligh–Dyer procedure. Different lipid species were separated by TLC [25]. The TLC plates were sprayed with scintillant and exposed to MP films. Signals were quantified using Image Gauge Version 3.3 from Fuji Photo Film Co, Ltd.

Sterol photo-cross-linking

COS7 cells were grown to subconfluence on 6 cm^2 dishes and transfected with OSBP/ORP expression plasmids as indicated in the Figure legends. [^{3}H]Photo-25OH (0.2 mCi of 20 Ci/mmol as ethanol solution) or [^{3}H]photoCH (0.2 mCi of 20 Ci/mmol solution complexed with β-methylcyclodextrin) was added 22 or 4 h after transfection respectively. Ethanol (0.5 %, v/v) in the medium was never exceeded. At 24 h after transfection cells were washed with ice-cold PBS and irradiated for 3 min using a 200 W high-pressure mercury lamp (Oriel Photomax, Stratford, CT, U.S.A.). Afterwards, cells were lysed with ice-cold lysis buffer (20 mM Hepes, pH 7.4, 100 mM NaCl, 5 mM EDTA, 1 % Triton X-100 and 0.5 % sodium deoxycholate) containing 0.5 mM PMSF and a protease inhibitor cocktail (Complete™ tablets; Roche, Mannheim, Germany). Cell lysates were incubated on a rotating wheel for 10 min at 4 °C followed by centrifugation at 15 700 ***g*** for 10 min at 4 °C. The supernatant was incubated for 3 h with monoclonal anti-Xpress antibody (Invitrogen) followed by incubation with Protein G–Sepharose beads for 16 h. Beads were washed four times with 20 mM Hepes (pH 7.25) and 0.5 % CHAPS and once with 100 mM Tris/HCl (pH 8.3), 150 mM NaCl, 2 mM EDTA, 0.1 % (w/v) SDS, 0.5 % (w/v) Nonidet P40 and 0.5 % (w/v) sodium deoxycholate. After washing, the proteins were eluted from the beads using reducing Laemmli sample buffer. While 1/10 of each sample was used to control for expression levels by SDS/PAGE/Western blotting, 9/10 was resolved on SDS/5–12 % PAGE gels, which were processed for fluorography.

Western blotting

Proteins were electrophoresed on Laemmli gels and electrotransferred to Hybond-C Extra nitrocellulose (GE Healthcare). Non-specific antibody binding was blocked with, and all antibody incubations were carried out in, 5 % (w/v) fat-free powdered milk in 10 mM Tris/HCl (pH 7.4), 150 mM NaCl and 0.05 % Tween 20. The bound Xpress antibody was visualized with horseradish-peroxidase-conjugated goat anti-mouse IgG (Bio-Rad) and the enhanced chemiluminescence system ECL® (GE Healthcare).

RESULTS

Binding of 25OH to ORP1 and ORP2 *in vitro*

We employed an *in vitro* [^{3}H]25OH binding assay with purified recombinant proteins to investigate sterol binding by human ORP1L [26], ORP1S and ORP2 [27], which were produced as GST fusions in *E. coli*. Since we failed to produce the GST fusion of rabbit OSBP ORD in soluble form, this protein was produced as an MBP fusion. The plain fusion partners, GST and MBP, were used as negative controls. To determine the specific 25OH binding, assays were performed in the presence and absence of a 40-fold excess of unlabelled 25OH. Both ORP1L and ORP1S, as well as ORP2, displayed specific 25OH binding (Figure 1). The affinities (apparent K_d) were determined by Scatchard analysis. The affinity determined for the MBP–OSBP ORD ($K_d = 7.8 \times 10^{-8}$ M) used as a positive control was lower than that previously reported for OSBP partially purified from mouse fibroblasts ($K_d = 3.9 \times 10^{-9}$ M; [28]). This could be due to production of the protein in the heterologous *E. coli* system as a fusion protein that has the N-terminal portion of the native OSBP replaced by MBP. The affinity of both the GST–ORP1L and GST–ORP1S variants for 25OH ($K_d = 9.7 \times 10^{-8}$ and 8.4×10^{-8} M respectively) was similar to that measured for MBP–OSBP ORD. The GST–ORP2 bound 25OH at markedly lower affinity ($K_d = 3.9 \times 10^{-6}$ M). The GST and MBP fusion partners used as negative controls did not show specific 25OH binding (results not shown). These results identify ORP1 and ORP2 as true OSBPs.

The structural model of human ORP2

We next wanted to investigate whether the observed 25OH binding occurs within a pocket similar to that reported for the yeast *S. cerevisiae* ORP Osh4p [16]. We have previously characterized human ORP2, and demonstrated functional effects of ORP2 overexpression on cholesterol, phospholipid and neutral lipid metabolism [11,12,27]. We therefore chose to model the structure of ORP2 using the yeast Osh4p structure as a template (Figure 2A). The overall sequence identity between ORP2 and the structural template Osh4p is approx. 23 %. The putative sterol-binding pocket exhibits a slightly higher degree of conservation than the rest of the protein. Major differences between the sequences of ORP2 and Osh4p include the N-terminal segment 1–62 and residues 339–393, which might form a loop or a small additional domain in ORP2. More than 80 % of the pocket-forming residues have similar polar or hydrophobic properties in both proteins. Only around Arg^{147} is the ORP2 pocket slightly more polar than its counterpart in Osh4p. This region is close to the D-ring of the sterol (Figure 2B). In some regions shifts in the sequence alignment may have positioned side chains incorrectly, but the model quality seemed sufficient to support site-directed mutagenesis by categorizing residues according to their potential function. For the present study we grouped residues as (i) ones that are part of the sterol-binding pocket and interact with the hydroxy head group, the quadruple ring structure or the aliphatic side chain of a sterol, (ii) ones that are not part of the pocket but might stabilize the fold, or (iii) ones that are exposed on the protein surface. Conservation in the sterol-binding pocket is higher than overall homology, but for some stretches, e.g. residues 233–240, the sequence alignment appeared less reliable. Therefore amino acid substitutions were mainly designed in regions where the sequence alignment/model quality is likely to be high. Amino acid residue Phe^{103}, which corresponds to Leu^{39} in Osh4p, is situated in the sterol-binding pocket close to the B-ring of 25OH (Figure 2B). Mutant F103W was intended to block sterol binding by steric hindrance. Lys^{150}, which corresponds to Lys^{109} in Osh4p, is located close to carbon-25 of the aliphatic side chain of sterols (Figure 2B). It was replaced by alanine (K150A), which creates more space and was expected to alter the affinity profile for different sterols as compared with the wt (wild-type) protein by removal of a charged amine. Ile^{249} is located close to C/D-rings of the sterol (Figure 2B) and corresponds to Val^{213} in Osh4p. Introducing a tryptophan residue in this position was expected to interfere sterically with sterol binding. Phe^{152} is located outside the sterol-binding pocket and corresponds to Leu^{111} in Osh4, which is supposed to stabilize the core fold of the protein [16]. This residue was replaced with aspartic acid residue (F152D). Met^{93} resides, according to the model, in the lid region of OPR2 close to the side chain hydroxy group of 25OH (Figure 2B). This residue

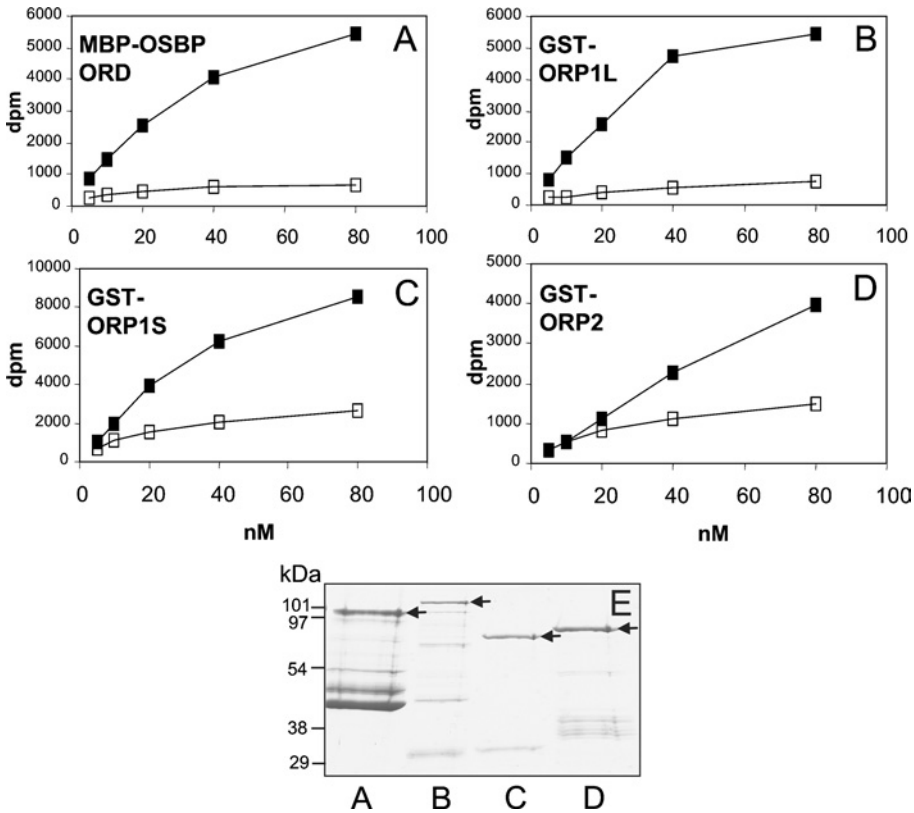

Figure 1 ORP1 and ORP2 bind 25OH *in vitro*

Binding of [^{3}H]25OH *in vitro* by (**A**) MBP–OSBP ORD (0.1 μM), (**B**) GST–ORP1L (1 μM), (**C**) GST–ORP1S (1 μM) and (**D**) GST–ORP2 (1 μM) fusion proteins was assayed as described in the Experimental section. The concentrations of the [^{3}H]sterol used are indicated at the bottom. The plots indicate the bound radioactivity (dpm) in the absence (closed symbols) and presence (open symbols) of competition by a 40-fold excess of unlabelled 25OH. The results shown are representative of two independent experiments with each protein. (**E**) Coomassie-stained Laemmli gel of the protein preparations used in (**A**–**D**). The full-length fusion proteins are indicated with arrows.

corresponds to Ala^{29} in Osh4p, and its replacement with a lysine residue (M93K) was predicted to modify sterol binding by ORP2.

The ORP2 mutants were produced as GST fusions in *E. coli* (Figure 2C) and their specific 25OH binding was tested by using the *in vitro* assay with 40 nM 25OH (Figure 2D). While the M93K, F152D and F103W mutations did not significantly impair the sterol interaction of ORP2, the K150A and I249W mutants displayed reduced 25OH binding (K150A, 70 % reduction, $P < 0.05$; I249W, 75 % reduction, $P < 0.01$). The reduced affinity of these mutants for 25OH resulted in signals too low for determination of K_d values by Scatchard analysis. These findings suggest that (i) the two residues are closely apposed to the bound sterol and (ii) ORP2 indeed contains a sterol-binding pocket as predicted by the model.

Labelling of COS7 cells with [^{3}H]photo-sterols

We next decided to use [^{3}H]photoCH and [^{3}H]photo-25OH (Figure 3A) to investigate the sterol interactions of the entire mammalian ORP family in live cells. The labelling of COS7 cells with these compounds should be carried out under conditions that allow maximal uptake of the [^{3}H]sterols and minimal metabolism. The conditions chosen (24 h incubation time for photoCH and 2 h for photo-25OH) represent a compromise between these two criteria. During these labelling periods approx. 40 % of photoCH and 30 % of photo-25OH were converted into esters (Figure 3B), most of them being available for protein interactions at membrane surfaces. During optimization of the labelling conditions we observed that increasing the labelling time with photo-25OH leads to a massive increase in ester formation: after 4 h approx. 60 % and after 24 h approx. 80 % of the photo-25OH were converted into esters (results not shown). Although the cells took up, under the labelling conditions used, approximately four times less photo-25OH than photoCH (Figure 3B), the total protein labelling was more pronounced with photo-25OH than with photoCH (Figure 3C), probably due to the fact that 25OH is more hydrophilic than cholesterol and thus desorbs from membranes at a higher rate, being more readily available for protein interactions.

Sterol binding by ORPs *in vivo*

We first expressed the ligand-binding ORDs of all ORPs, fused with an N-terminal Xpress epitope tag, in COS7 cells and performed photoaffinity labelling using [^{3}H]photo-25OH (Figure 4A) and [^{3}H]photoCH. While none of the proteins bound detectable amounts of photoCH (therefore omitted from Figure 4A), ORP1S (=ORP1 ORD), ORP2 (=ORP2 ORD) and the ORDs of ORP4, ORP7 and ORP10 bound photo-25OH. The ORDs of OSBP, ORP3, ORP5, ORP6, ORP8, ORP9 and ORP11 failed to show detectable signal with photo-25OH, or displayed weak binding in only some experiments (Figure 4A; Table 1). We suspected that the lack of binding might be a consequence of a predominantly cytosolic distribution of the truncated ORD proteins, which lack N-terminal membrane-targeting determinants [26,29–31]. Therefore we repeated the labelling experiment using tagged full-length constructs of all

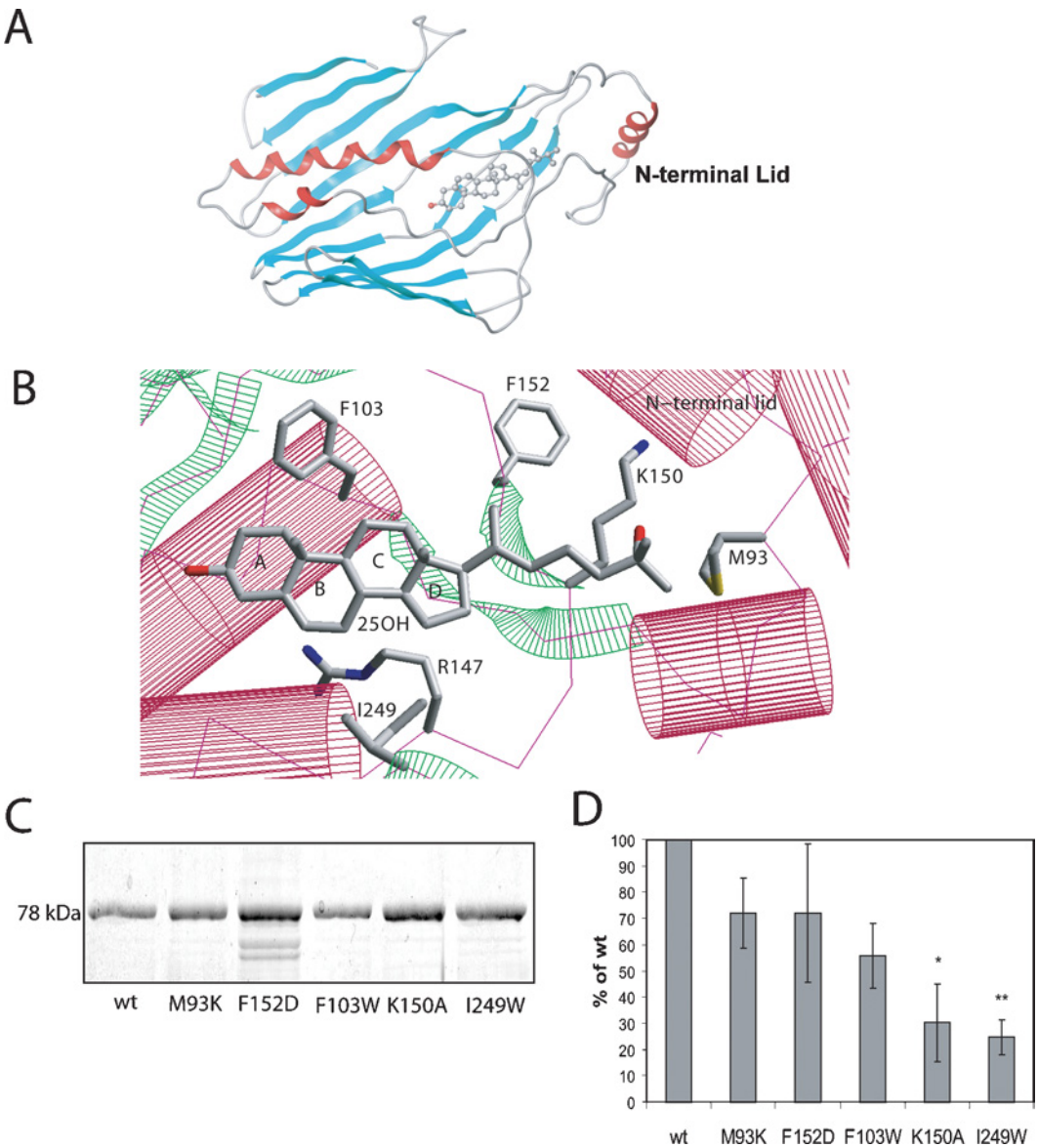

Figure 2 Sterol binding to ORP2

(**A**) The structure of ORP2 amino acid region 63–338, containing the ligand-binding site, was modelled using the structure of the yeast homologue Osh4p as a template. The structure consists of an array of antiparallel β-strands (blue) that form a groove in which the sterol ligand is inserted. This groove is closed by a lid structure that is formed by α-helices (red) in the N-terminal part of the sequence. The co-ordinates of the structural model are available from the authors upon request. (**B**) A detailed view of the ligand-binding site containing a molecule of 25OH. Only side chains of selected residues that come close to the sterol are shown (M93, F103, R147, K150, F152 and I249). These residues, except R147, were selected for mutational analysis of sterol binding. (**C**) Coomassie-stained Laemmli gel of the wt and mutant GST–ORP2 preparations used for the binding assays in the next panel. (**D**) Specific 25OH binding by the ORP2 mutants *in vitro* was assayed using 1 μM protein and 40 nM 25OH. The bars represent specific binding, % of that by wt ORP2. The results are representative of three independent experiments each performed in quadruplicate (means $\pm$ S.E.M.; $^{*}P < 0.05$ and $^{**}P < 0.01$, as determined by Student's *t* test).

ORPs except ORP4 and ORP5. Instead of full-length ORP5 we used here an ORD construct extended to contain the putative transmembrane anchor. Very strong labelling was detected for ORP1L and full-length ORP8, strong labelling for ORP3, ORP5 and ORP10, and weak labelling for OSBP, ORP6 and ORP11 (Figure 4B; Table 1). Interestingly, ORP1L showed strong binding of photoCH, and reproducible cross-linking of photoCH was also detected for ORP3, ORP5 and ORP8 (Figure 4B; Table 1). A truncated version of ORP1L lacking the ORD (ORP1L ΔORD) bound neither photo-25OH nor photoCH, evidencing that the observed binding is specific and occurs within the ORD. The ORP1L ΔORD protein was shown to localize correctly on late endocytic compartments (results not shown), similar to the full-length ORP1L [26,32].

DISCUSSION

ORPs are a family of sterol-binding proteins

In the present study we employed both an *in vitro* sterol-binding assay and photo-cross-linking in live cells to investigate the interactions of mammalian ORPs with sterols. The *in vitro* results demonstrate that both ORP1 and ORP2 show specific 25OH binding, identifying them for the first time as true OSBPs.

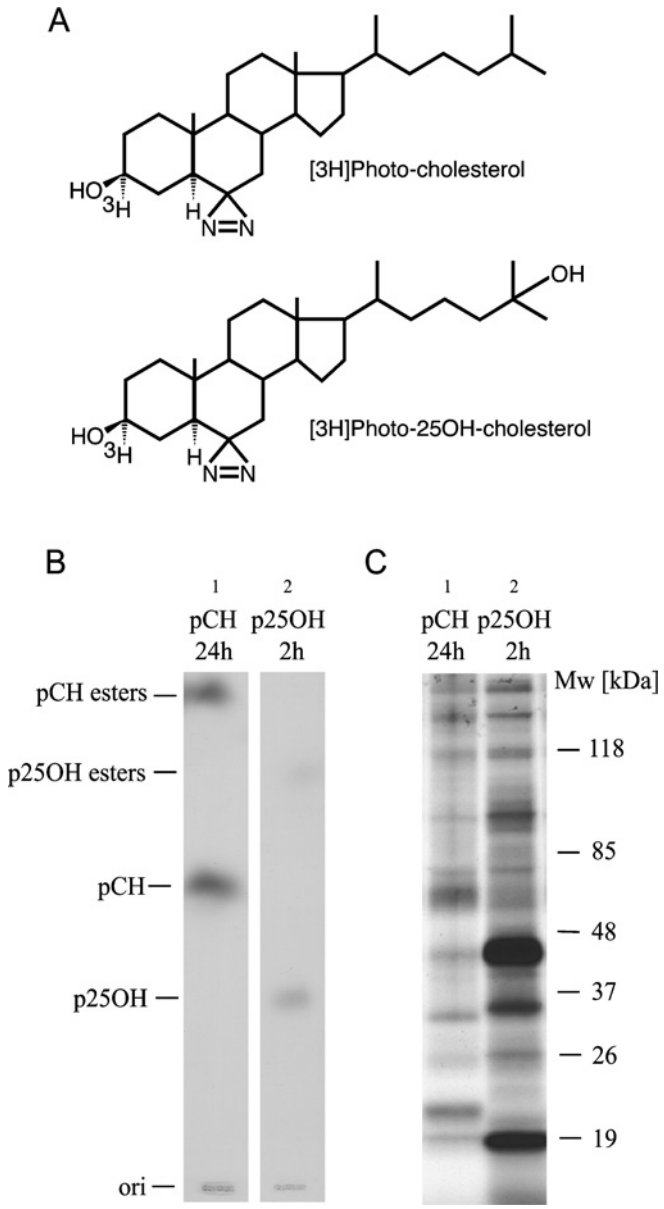

Figure 3 Metabolism of [^{3}H]photoCH and [^{3}H]photo-25OH in COS7 cells

(**A**) Structures of [^{3}H]photoCH and [^{3}H]photo-25OH. (**B**, **C**) COS7 cells were grown for 20 h in the presence of 0.2 mCi of [^{3}H]photoCH complexed with cyclodextrin (pCH; lane 1) or for 2 h in the presence of 0.2 mCi of an ethanolic solution of [^{3}H]photo-25OH (p25OH; lane 2). After UV-induced cross-linking cellular lipids were extracted with chloroform/methanol and separated by TLC (**B**), and proteins in total cellular lysates were analysed by SDS/PAGE followed by fluorography (**C**).

The live cell photo-cross-linking suggests that, in addition to ORP1 and ORP2, most of the other family members also show affinity for 25OH. In addition, ORP1L, ORP3, ORP5 and ORP8 showed affinity for photoCH. In total, we present evidence for sterol interaction by 11 members of the ORP family. Thus ORPs may constitute the largest family of sterol-binding proteins. The StAR (steroidogenic acute regulatory protein)-related proteins are a lipid-binding protein family comprising 15 members that show, similar to the ORP family, a modular composition with a conserved lipid-binding domain and various additional protein modules [33]. Proteins of this family bind a diverse set of lipid ligands: cholesterol, phosphatidylcholine, phosphatidylethanolamine and ceramide. In contrast, it seems that most of the ORPs are able to bind sterols, although the degree of sequence conservation within their ORD domains is not particularly high, ranging from 18 to 85 % [4]. Furthermore, this property is conserved from the evolutionary distant yeast *S. cerevisiae* Osh4p [16]. A striking feature of the sterol binding by Osh4p is that only few amino acid residues in the sterol-binding pocket make direct contacts with the bound sterol, but the ligand interaction mainly occurs via contacts with ordered water molecules [16]. This arrangement should give the binding site sufficient flexibility to host other lipidic ligands, possibly also of larger size or increased hydrophilicity. In fact, Osh4p was reported to be able to transfer, in addition to sterols, also certain phospholipids [15]. To test if mammalian ORPs could bind phospholipids we performed photolabelling with derivatives of phosphatidylcholine and sphingomyelin, but could not detect any cross-linking to ORPs (Table 1). It should, however, be noticed that the set of ligands used in our study is far from complete. It might well be that the natural ligands for some of the ORPs are neither cholesterol nor 25OH, but other oxysterols, a variety of which are present in mammalian tissues [34]. Furthermore, the present results do not exclude the possibility that some phospholipids may interact with the ORP ligand-binding pocket.

The photo-sterols used differ slightly in structure from their native counterparts (Figure 3). This has to be kept in mind when interpreting the results obtained by photo-cross-linking: the strength of signals obtained for the different ORPs does not necessarily reflect the order of their relative affinities for native 25OH. Furthermore, the subcellular localization/membrane association of the expressed proteins is likely to affect the results obtained by live cell photo-cross-linking. In several cases the truncated ORDs failed to cross-link detectably to photo-25OH, while the corresponding full-length proteins displayed a positive signal. This is probably due to the fact that the full-length proteins carry membrane-targeting determinants not present in the ORDs [26,29–31], and efficient membrane association is likely to enhance the ligand acquisition. It should especially facilitate binding of cholesterol or keto-sterols relative to the more polar hydroxylated sterols that can probably bind directly from a soluble pool. A predominantly cytosolic distribution would also provide a plausible explanation to the puzzling finding that the ORD of OSBP bound 25OH quite well *in vitro*, but showed no signal in the photo-cross-linking assay.

Sterols bind to the ligand-binding domain

The combination of molecular modelling and mutational analysis of sterol binding allowed the conclusion that sterol binding to ORP2, and possibly to the other family members as well, occurs within a similar binding pocket to that identified in yeast Osh4p by X-ray crystallographic analysis [16]. Recently, PIP binding was described for short linear sequences of the ORP1 ligand-binding domain [19]. Furthermore, binding of negatively charged phospholipids has been reported for ORP2, ORP9 and ORP10 [11,18,20]. The analysis by Im et al. [16] and Raychaudhuri et al. [15] suggested that charged residues near the entrance of the sterol-binding pocket interact with acidic phospholipids, especially PIPs, on membrane surfaces and are crucial for Osh4p function. These residues are conserved between Osh4p and ORP2, consistent with the observed interaction of ORP2 with phospholipid vesicles containing PIPs [11]. It remains to be solved if the PIP interaction involves binding into the actual ORP ligand-binding pocket or just head group interactions with charged determinants on the protein surface.

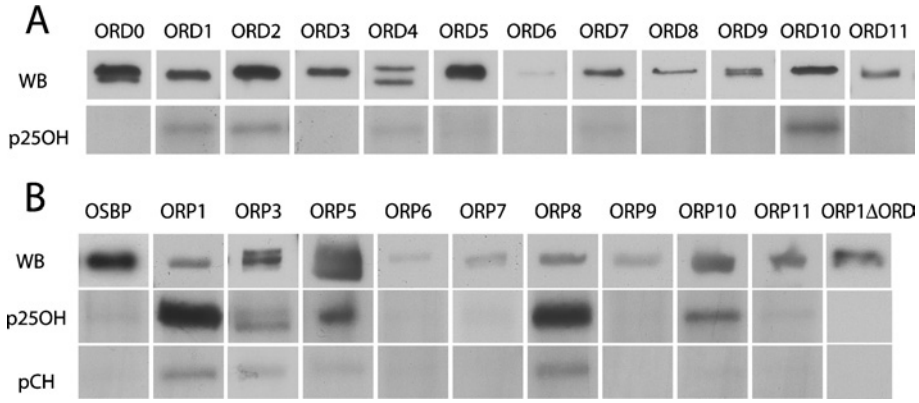

Figure 4 Sterol binding by ligand-binding domains and full-length ORP proteins

COS7 cells were transfected with epitope-tagged ligand-binding domains (ORD) of OSBP (ORD0) or ORP1–11 (ORD1–11) (**A**) or full-length proteins (**B**). Photo-cross-linking with photoactivatable derivatives of 25OH (p25OH) or cholesterol (pCH) was performed as described in the Experimental section, and the ORP proteins were immunoprecipitated, followed by SDS/PAGE and fluorography. The amounts of the proteins in the precipitates were visualized by Western blotting (WB). ORP2 is missing from (**B**) since it is a short protein consisting of the ORD only. The results shown are representative of at least three independent experiments performed with each protein.

Table 1 Photo-cross-linking of lipids to ORDs and full-length ORP proteins

Arbitrary scale (0–10), based on quantification of the cross-linking signals relative to the Western blot signals. +++, Very strong signal (5–10); ++, strong signal (3–5); +, weak signal (1–3); +/–, weak signal observed only in some experiments; –, no signal; NE, not evaluated. The results are based on at least three independent experiments performed with each protein.

(a)

	ORD0*	ORD1	ORD2	ORD3	ORD4	ORD5	ORD6	ORD7	ORD8	ORD9	ORD10	ORD11
p25OH†	+/–	+	++	+/–	+	+/–	–	+	–	–	+	–
pCH‡	–	–	+/–	–	–	–	–	+/–	–	–	–	–

(b)

	OSBP	ORP1	–	ORP3	–	ORP5§	ORP6	ORP7	ORP8	ORP9	ORP10	ORP11
p25OH	+	+++		++		++	+	+/–	+++	+/–	++	+
pCH	+/–	++		+		+	+/–	+/–	+	–	+/–	+/–
pPC‖	–	NE		NE		NE	–	–	NE	–	–	–
pSM¶	–	NE		NE		NE	–	–	NE	–	–	–

* The ORD of OSBP; ORD1–11 represent the ORDs of ORP1–11 respectively.
† Photo-25OH.
‡ PhotoCH.
§ ORP5 indicates ORD extended with the putative C-terminal transmembrane anchor.
‖ Photo-phosphatidylcholine.
¶ Photo-sphingomyelin.

The present study does not allow us to conclude whether ORPs act as sterol transporters [15] or transmitters of sterol signals, as suggested for OSBP [9,10]. However, our work suggests that ORPs constitute the largest family of intracellular sterol-binding proteins with functions in lipid metabolism, intracellular lipid transport, membrane trafficking and cell signalling.

We thank Seija Puomilahti and Pirjo Ranta for skilled technical assistance. This study was supported by the Academy of Finland (grants 206298, 113013 and 118720 to V. M. O.), the Sigrid Jusélius Foundation, the Finnish Foundation for Cardiovascular Research and the Finnish Society of Sciences and Letters (V. M. O.).

REFERENCES

1 Lehto, M. and Olkkonen, V. M. (2003) The OSBP-related proteins: a novel protein family involved in vesicle transport, cellular lipid metabolism, and cell signalling. Biochim. Biophys. Acta **1631**, 1–11
2 Olkkonen, V. M. (2004) Oxysterol binding protein and its homologues: new regulatory factors involved in lipid metabolism. Curr. Opin. Lipidol. **15**, 321–327
3 Beh, C. T., Cool, L., Phillips, J. and Rine, J. (2001) Overlapping functions of the yeast oxysterol-binding protein homologues. Genetics **157**, 1117–1140
4 Lehto, M., Laitinen, S., Chinetti, G., Johansson, M., Ehnholm, C., Staels, B., Ikonen, E. and Olkkonen, V. M. (2001) The OSBP-related protein family in humans. J. Lipid Res. **42**, 1203–1213
5 Anniss, A. M., Apostolopoulos, J., Dworkin, S., Purton, L. E. and Sparrow, R. L. (2002) An oxysterol-binding protein family identified in the mouse. DNA Cell Biol. **21**, 571–580
6 Lagace, T. A., Byers, D. M., Cook, H. W. and Ridgway, N. D. (1999) Chinese hamster ovary cells overexpressing the oxysterol binding protein (OSBP) display enhanced synthesis of sphingomyelin in response to 25-hydroxycholesterol. J. Lipid Res. **40**, 109–116
7 Lagace, T. A., Byers, D. M., Cook, H. W. and Ridgway, N. D. (1997) Altered regulation of cholesterol and cholesteryl ester synthesis in Chinese-hamster ovary cells overexpressing the oxysterol-binding protein is dependent on the pleckstrin homology domain. Biochem. J. **326**, 205–213
8 Nishimura, T., Inoue, T., Shibata, N., Sekine, A., Takabe, W., Noguchi, N. and Arai, H. (2005) Inhibition of cholesterol biosynthesis by 25-hydroxycholesterol is independent of OSBP. Genes Cells **10**, 793–801

9 Perry, R. J. and Ridgway, N. D. (2006) Oxysterol-binding protein and vesicle-associated membrane protein-associated protein are required for sterol-dependent activation of the ceramide transport protein. Mol. Biol. Cell **17**, 2604–2616

10 Wang, P. Y., Weng, J. and Anderson, R. G. (2005) OSBP is a cholesterol-regulated scaffolding protein in control of ERK 1/2 activation. Science **307**, 1472–1476

11 Hynynen, R., Laitinen, S., Käkelä, R., Tanhuanpää, K., Lusa, S., Ehnholm, C., Somerharju, P., Ikonen, E. and Olkkonen, V. M. (2005) Overexpression of OSBP-related protein 2 (ORP2) induces changes in cellular cholesterol metabolism and enhances endocytosis. Biochem. J. **390**, 273–283

12 Käkelä, R., Tanhuanpää, K., Laitinen, S., Somerharju, P. and Olkkonen, V. M. (2005) Overexpression of OSBP-related protein 2 (ORP2) in CHO cells induces alterations of phospholipid species composition. Biochem. Cell Biol. **83**, 677–683

13 Wang, C., JeBailey, L. and Ridgway, N. D. (2002) Oxysterol-binding-protein (OSBP)-related protein 4 binds 25-hydroxycholesterol and interacts with vimentin intermediate filaments. Biochem. J. **361**, 461–472

14 Beh, C. T. and Rine, J. (2004) A role for yeast oxysterol-binding protein homologs in endocytosis and in the maintenance of intracellular sterol-lipid distribution. J. Cell Sci. **117**, 2983–2996

15 Raychaudhuri, S., Im, Y. J., Hurley, J. H. and Prinz, W. A. (2006) Nonvesicular sterol movement from plasma membrane to ER requires oxysterol-binding protein-related proteins and phosphoinositides. J. Cell Biol. **173**, 107–119

16 Im, Y. J., Raychaudhuri, S., Prinz, W. A. and Hurley, J. H. (2005) Structural mechanism for sterol sensing and transport by OSBP-related proteins. Nature **437**, 154–158

17 Taylor, F. R., Saucier, S. E., Shown, E. P., Parish, E. J. and Kandutsch, A. A. (1984) Correlation between oxysterol binding to a cytosolic binding protein and potency in the repression of hydroxymethylglutaryl coenzyme A reductase. J. Biol. Chem. **259**, 12382–12387

18 Fairn, G. D. and McMaster, C. R. (2005) The roles of the human lipid-binding proteins ORP9S and ORP10S in vesicular transport. Biochem. Cell Biol. **83**, 631–636

19 Fairn, G. D. and McMaster, C. R. (2005) Identification and assessment of the role of a nominal phospholipid binding region of ORP1S (oxysterol-binding-protein-related protein 1 short) in the regulation of vesicular transport. Biochem. J. **387**, 889–896

20 Xu, Y., Liu, Y., Ridgway, N. D. and McMaster, C. R. (2001) Novel members of the human oxysterol-binding protein family bind phospholipids and regulate vesicle transport. J. Biol. Chem. **276**, 18407–18414

21 Thiele, C., Hannah, M. J., Fahrenholz, F. and Huttner, W. B. (2000) Cholesterol binds to synaptophysin and is required for biogenesis of synaptic vesicles. Nat. Cell Biol. **2**, 42–49

22 Adams, C. M., Reitz, J., De Brabander, J. K., Feramisco, J. D., Li, L., Brown, M. S. and Goldstein, J. L. (2004) Cholesterol and 25-hydroxycholesterol inhibit activation of SREBPs by different mechanisms, both involving SCAP and Insigs. J. Biol. Chem. **279**, 52772–52780

23 Thompson, J. D., Higgins, D. G. and Gibson, T. J. (1994) CLUSTAL W: improving the sensitivity of progressive multiple sequence alignment through sequence weighting, position-specific gap penalties and weight matrix choice. Nucleic Acids Res. **22**, 4673–4680

24 Taylor, F. R. and Kandutsch, A. A. (1985) Use of oxygenated sterols to probe the regulation of 3-hydroxy-3-methylglutaryl-CoA reductase and sterologenesis. Methods Enzymol. **110**, 9–19

25 Kuerschner, L., Ejsing, C. S., Ekroos, K., Shevchenko, A., Anderson, K. I. and Thiele, C. (2005) Polyene-lipids: a new tool to image lipids. Nat. Methods **2**, 39–45

26 Johansson, M., Bocher, V., Lehto, M., Chinetti, G., Kuismanen, E., Ehnholm, C., Staels, B. and Olkkonen, V. M. (2003) The two variants of oxysterol binding protein-related protein-1 display different tissue expression patterns, have different intracellular localization, and are functionally distinct. Mol. Biol. Cell **14**, 903–915

27 Laitinen, S., Lehto, M., Lehtonen, S., Hyvärinen, K., Heino, S., Lehtonen, E., Ehnholm, C., Ikonen, E. and Olkkonen, V. M. (2002) ORP2, a homolog of oxysterol binding protein, regulates cellular cholesterol metabolism. J. Lipid Res. **43**, 245–255

28 Kandutsch, A. A. and Shown, E. P. (1981) Assay of oxysterol-binding protein in a mouse fibroblast, cell-free system. Dissociation constant and other properties of the system. J. Biol. Chem. **256**, 13068–13073

29 Lehto, M., Hynynen, R., Karjalainen, K., Kuismanen, E., Hyvärinen, K. and Olkkonen, V. M. (2005) Targeting of OSBP-related protein 3 (ORP3) to endoplasmic reticulum and plasma membrane is controlled by multiple determinants. Exp. Cell Res. **310**, 445–462

30 Ridgway, N. D., Dawson, P. A., Ho, Y. K., Brown, M. S. and Goldstein, J. L. (1992) Translocation of oxysterol binding protein to Golgi apparatus triggered by ligand binding. J. Cell Biol. **116**, 307–319

31 Wyles, J. P. and Ridgway, N. D. (2004) VAMP-associated protein-A regulates partitioning of oxysterol-binding protein-related protein-9 between the endoplasmic reticulum and Golgi apparatus. Exp. Cell Res. **297**, 533–547

32 Johansson, M., Lehto, M., Tanhuanpää, K., Cover, T. L. and Olkkonen, V. M. (2005) The oxysterol-binding protein homologue ORP1L interacts with Rab7 and alters functional properties of late endocytic compartments. Mol. Biol. Cell **16**, 5480–5492

33 Alpy, F. and Tomasetto, C. (2005) Give lipids a START: the StAR-related lipid transfer (START) domain in mammals. J. Cell Sci. **118**, 2791–2801

34 Björkhem, I. and Diczfalusy, U. (2002) Oxysterols: friends, foes, or just fellow passengers? Arterioscler. Thromb. Vasc. Biol. **22**, 734–742

Received 1 February 2007/4 April 2007; accepted 11 April 2007
Published as BJ Immediate Publication 11 April 2007, doi:10.1042/BJ20070176